Published in final edited form as:

Neuroimage. 2019 January 15; 185: 479–489. doi:10.1016/j.neuroimage.2018.10.024.

The Neural Architecture of Executive Functions Is Established by Middle Childhood

Laura E. Engelhardt[1], **K. Paige Harden**[1,2], **Elliot M. Tucker-Drob**[1,2], and **Jessica A. Church**[1,3]

[1]Department of Psychology, The University of Texas at Austin

[2]Population Research Center, The University of Texas at Austin

[3]Imaging Research Center, The University of Texas at Austin

Abstract

Executive functions (EFs) are regulatory cognitive processes that support goal-directed thoughts and behaviors and that involve two primary networks of functional brain activity in adulthood: the fronto-parietal and cingulo-opercular networks. The current study assessed whether the same networks identified in adulthood underlie child EFs. Using task-based fMRI data from a diverse sample of $N = 117$ children and early adolescents (M age = 10.17 years), we assessed the extent to which neural activity was shared across switching, updating, and inhibition domains, and whether these patterns were qualitatively consistent with adult EF-related activity. Brain regions that were consistently engaged across switching, updating, and inhibition tasks closely corresponded to the cingulo-opercular and fronto-parietal networks identified in studies of adults. Isolating brain activity during more demanding task periods highlighted contributions of the dorsal anterior cingulate and anterior insular regions of the cingulo-opercular network. Results were independent of age and time-on-task effects. These results indicate that the two core brain networks that support EFs are in place by middle childhood, in agreement with resting-state findings of adultlike brain network organization. Improvement in EFs from middle childhood to adulthood, therefore, are likely due to quantitative changes in activity within these networks, rather than qualitative changes in the organization of the networks themselves. Improved knowledge of how the brain's functional organization supports EF in childhood has critical implications for understanding the maturation of cognitive abilities.

Graphical Abstract

Corresponding author: Laura E. Engelhardt, 108 E Dean Keeton St., Stop A8000, Austin, TX 78712 512-471-2221, le2241@gmail.com.

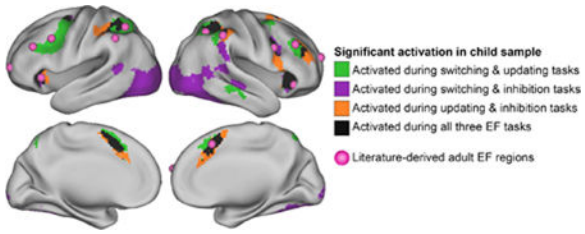

Keywords

Executive function; children; fMRI; cingulo-opercular network; fronto-parietal network

Introduction

Cognitive maturation involves transitioning from stimulus-driven and reflexive actions to more deliberate thoughts and behaviors (Luna et al., 2004; Rueda et al., 2004; Thelen, 1995). Executive functions (EFs) - regulatory processes that monitor goal-directed cognitive operations - are critical for the developmental transition to adultlike thoughts and behaviors. Because of the importance of EFs for psychiatric health and cognitive skill formation in both childhood and adulthood (Best et al., 2011; Buckner, 2004; Salthouse et al., 2003; Zelazo and Müller, 2002), neuroscientists have been interested in understanding the neural mechanisms underlying normative maturation in EFs (Aron, 2008; Banich, 2009). An exciting open question in this area is how the brain changes over development to support better performance across a variety of executive domains.

Neural Architecture and Factor Structure of Executive Functions in Adulthood

Substantial individual differences and developmental differences are evident across separable EF domains, which include (a) *response inhibition,* or the ability to refrain from executing a practiced response; (b) *switching,* which requires performance adaptations in response to changing rules or goals; and (c) *updating,* which involves replacing information in working memory based on new demands (for reviews, see Best and Miller, 2010; Diamond, 2002; Huizinga et al., 2006). Although these domains are statistically distinguishable, they also covary strongly, suggesting that domain-general executive resources underlie ability in any one specific domain. This pattern of relationships between EF domains is often referred to as the “unity and diversity” model (Miyake et al., 2000).

Consistent with the “unity” of adult EFs, neuroimaging studies in adulthood have identified a core set of brain networks that are consistently activated in response to an array of tasks tapping different EF domains. Lesion studies and early functional magnetic resonance imaging (fMRI) work provided initial evidence that the prefrontal cortex (PFC) was fundamental to attention, working memory, and inhibition (for a review, see Collette et al., 2006). More recent investigations employing multiple tasks have uncovered complex and distributed networks of brain regions active during EF tasks. Specifically, the *fronto-parietal network* includes bilateral inferior or middle frontal gyrus (IFG, MFG), dorsolateral prefrontal cortex (dlPFC), inferior parietal lobule (IPL), superior parietal lobule (SPL), and pre-motor areas (Cacioppo et al., 1984; Collette et al., 2006; Congdon et al., 2010; Nee et

al., 2012; Niendam et al., 2012; Owen et al., 2005), and the *cingulo-opercular network* includes dorsal anterior cingulate cortex (dACC) and bilateral anterior insula and is reliably active during error processing and task maintenance (Dosenbach et al., 2006, 2008, 2007; Menon and Uddin, 2010).

Resting-state fMRI analyses suggest that findings from EF task-based studies identify networks of regions that are also intrinsically connected, as region-to-region correlations in spontaneous BOLD activity also cluster into dissociable fronto-parietal and cingulo-opercular networks across many samples (Crittenden et al., 2016; Dosenbach et al., 2007; Power et al., 2011; Yeo et al., 2011). Overall, neuroimaging studies of adults have revealed a highly consistent set of regions that co-activate in response to executive demands. This detailed characterization sets a standard for evaluating the consistency of children's EF-related brain activation.

From Childhood to Adulthood: Qualitative or Quantitative Changes?

When does this core set of brain regions develop to support EF task performance? Empirical results that answer this question will undoubtedly inform the design and evaluation of interventions to support children with EF deficits. One possible mechanism for age-related improvements in EF is that the networks of regions that support optimal deployment of executive function are not yet in place in childhood and that the maturation of EF results from the progressive establishment of an adultlike EF network over development. Support for such a *qualitative* account would come from findings that patterns of brain activity during executively demanding tasks are more diffuse among children or entirely distinct from patterns observed among adults. One example of qualitative, age-related changes in neural organization is early visually guided behaviors, which initially rely on subcortical activity before transitioning to predominantly posterior, and then anterior, cortical activation (Johnson, 1990). Alternatively, a relatively consistent set of brain regions might undergo *quantitative* maturation before reaching their apex in adolescence or adulthood. This account of brain-behavior development would reflect strengthening or refinement of region-to-region connections and would be evidenced by engagement of a consistent set of brain regions across developmental stages (Johnson, 2001; 2011). Declarative memory, for example, is mediated by activation in the medial temporal lobes and PFC from childhood through adulthood, with memory enhancement linked to age-related differences in the strength - but not location - of BOLD activity (Ofen et al., 2007).

Behavioral studies of the factor structure of EF performance in childhood provide indirect support for quantitative maturation, i.e., that the neural architecture underlying successful engagement of executive resources is in place by middle childhood. Notably, the "unity and diversity" model seen in adults, with a highly heritable factor that contributes to EF ability across domains and tasks (Miyake et al., 2000), is evident as early as 8 years old (Engelhardt et al., 2015). This suggests that common causal processes act on individual EFs in childhood, which is consistent with reliable, cross-task brain activity observed in adults.

Additionally, neuroimaging studies of EFs in childhood have found that individual tasks consistently engage temporal cortex, parietal cortex, and subcortical regions (e.g., Bunge and Wright, 2007; Church et al., 2017; Crone and Dahl, 2012; Ordaz et al., 2013; Yaple and

Arsalidou, 2018). In conjunction with resting-state analyses (Power et al., 2012), single-domain studies highlight children's engagement of the fronto-parietal and cingulo-opercular regions described above. However, a major limitation of neuroimaging studies of childhood EFs is that they typically employ only a single EF task. Consequently, it is difficult to generalize findings across samples employing different tasks and to identify the extent to which task-related brain activity is task- or domain-specific versus general across EF domains.

To date, meta-analyses of children's fMRI data have been the only avenue for addressing these questions. An early meta-analysis of 25 studies found evidence for consistent activation of bilateral prefrontal cortex, bilateral insula, and left parietal regions across tasks and age, as well as age-related changes in the lateralization of insula activity during individual EF tasks (Houde et al., 2010). More recently, a meta-analysis of 53 studies of single EF tasks found evidence for cross-domain engagement of bilateral frontal, bilateral insula, and right parietal clusters, as well as evidence for domain-specific activation during switching and updating tasks (McKenna et al., 2017). The regions identified in meta-analysis are largely consistent with the adult "core control system" described by Dosenbach and colleagues (2006, 2007), though with less consistency regarding the contribution of parietal regions.

However, meta-analyses cannot completely control for between-samples differences that may confound the results. For example, the greater number of studies examining the updating and inhibition domains, relative to the switching domain, may have biased previous findings regarding the relationships between these core constructs (McKenna et al., 2017). This work has not been able to directly test for adultlike functional EF networks within the same group of individuals or across evenly represented domains. Thus, previous single-task studies and meta-analyses provide *circumstantial* evidence suggesting that children activate a common set of brain regions during a variety of EF tasks and that these regions are the same as those activated by adults.

Goals and Methodological Advantages of the Current Study

The goal of the current study was to provide the first direct test of whether the common neural architecture of EFs seen in adulthood is present by middle childhood. We hypothesized that the same functional brain networks that have been implicated in the adult literature (i.e., fronto-parietal and cingulo-opercular networks) would activate across three tasks tapping three distinct EF domains: switching, inhibition, and updating. To address this goal, we measured neural response to three EF tasks in a large, population-representative, and well characterized sample of children. This approach has several methodological advantages over previous meta- analytic approaches, including (a) the removal of between-study differences as a source of confounding variance; (b) the ability to apply greater quality control methods, including performance-based exclusionary criteria to isolate EF-related from non-EF-related activity; and (c) the ability to control for performance differences that may impact task-related fMRI signals. This is important because trial-by-trial variation in response time (RT), or "time-on-task" effects, positively corresponds to activation in regions implicated in EFs, such as bilateral insula and right dlPFC (Yarkoni et al., 2009). We

addressed this issue by controlling for time-on-task effects at the whole-brain level and by separately examining the BOLD correlates of RT across tasks. Finally, we were able to conduct a formal comparison of activity in our sample to *a priori* regions defined by the adult literature.

Materials and Methods

Participants

As part of the neuroimaging arm of the Texas Twin Project (Harden et al., 2013), 127 twins or multiples in 3rd through 8th grade participated in an MRI session. Ten participants were excluded from the analyses due to incidental findings ($N = 1$), equipment malfunction ($N = 2$), refusal to continue ($N = 3$), or failure to meet movement and performance cutoffs across all collected tasks ($N = 4$). The final sample consisted of 117 participants with mean age of 10.17 years ($SD = 1.37$, range = 7.96 to 13.85); 57 participants were female. Participants reported diverse racial and ethnic backgrounds: 43.6% were non-Hispanic white, 14.5% were Hispanic, 5.1% were African American, 5.1% were Asian, 1.7% were another race, and 29.9% reported multiple races or ethnicities. The sample comprised 52 twin pairs (21 monozygotic, 16 same-sex dizygotic, and 15 opposite-sex dizygotic) and 13 individuals whose co-twins were not scanned. Zygosity was determined by a latent class analysis of researchers' and parents' ratings of twins' physical similarity. The current study does not examine twin relations.

Developmental or learning disorder diagnoses were reported by parents for eight participants. Six participants had attention deficit hyperactivity disorder, one of whom also reported non-specific reading disability; two had Asperger syndrome; and one had dyslexia. Four of the participants that reported a diagnosis had taken neurostimulant medication the day of scanning; another participant had taken a selective serotonin reuptake inhibitor and an adrenergic agonist. Results of the primary analyses with and without these individuals are described below.

MRI Data Acquisition

All procedures followed the human subjects research regulations overseen by the University of Texas at Austin Institutional Review Board. Twins were scanned consecutively on the same day. Parents provided informed consent for their children's participation, and participants provided informed assent. Participants were compensated for their time. Images were acquired on a Siemens Skyra 3-Tesla scanner with a 32-channel head matrix coil. We collected T1-weighted structural images with an MPRAGE sequence (TR = 2530 ms, TE = 3.37 ms, FOV = 256, 1×1×1mm voxels), as well as T2-weighted structural images with a turbo spin echo sequence (TR = 3200 ms, TE = 412 ms, FOV = 250, 1×1×1mm voxels). During tasks, we collected functional images using a multi-band echo-planar sequence (TR = 2000 ms, TE = 30 ms, flip angle = 60°, multiband factor = 2, 48 axial slices, 2×2×2mm voxels, base resolution = 128×128). Tasks were run on PsychoPy version 1.8 (Peirce, 2007); stimuli were projected at a resolution of 1920×1080 to a screen that participants viewed via a mirror attached to the head coil. Participants wore Optoacoustics headphones and provided responses using a two-button response pad.

fMRI Tasks

Task order was fixed to maximize the likelihood of retaining usable data across EF domains, and to avoid confounding sequence effects with individual differences (Tucker-Drob, 2011). Tasks were ordered as follows: resting state (not presented here), switching task, updating task, inhibition task, switching task, updating task, resting state. The total scan time was approximately 1.25 hours.

Switching task.—Participants performed up to two runs of a cued switching task (Supplementary Figure 1a; Baym et al., 2008). Runs consisted of 46 trials in which participants were cued to pay attention to the shape or color of a target stimulus that would appear later. The two possible rules (shape and color) and two responses choices were displayed for the duration of the trial. A red box indicating which rule to follow appeared for the first 1.5 seconds of the trial. On 37 of the 46 trials, the target stimulus appeared .5 seconds after the red box disappeared, and the target remained on the screen for 2 seconds, during which time the participant could indicate which of the response choices matched the target. The response period was followed by a 1 second fixation cross. In 9 trials interspersed throughout the run, a target did not appear and a red fixation cross was displayed for .5 seconds, followed by a white fixation cross for .5 seconds. The cue-only trials allowed us to separate neural signals during the cue period from those during the target stimulus period (Ollinger et al., 2001). All trials were followed by a jitter of 0–8 seconds. The total run time was 5 minutes and 22 seconds. In the first run, the cued rule was consistent with the previous rule on 22 trials (repeat trial), and these were interspersed with 23 trials where the cued rule switched (switch trial). In the second run, there were 23 repeat rule trials, and 22 switch rule trials.

Updating task.—Participants completed up to two runs of an N-back task (Supplementary Figure 1b; adapted from Jaeggi et al., 2010). Each run consisted of 64 shape stimuli evenly divided into a 1-back and 2-back block. Block order was fixed. Prior to each block, participants viewed an instruction picture for 4 seconds that indicated whether they should look for shapes that matched one shape prior (1-back) or two shapes prior (2-back). During the blocks, each stimulus appeared for 1.5 seconds, followed by a 1 second inter-stimulus interval. Participants pressed a button when they believed the stimulus matched one or two shapes prior, according to the block-specific instructions. A 20 second fixation followed each block. Each block had a total of 7 matches (21.9% of trials). Updating runs lasted 3 minutes and 32 seconds.

Inhibition task.—To assess response inhibition, we administered one run of a visual Stop Signal task (Supplementary Figure 1c; Verbruggen and Logan, 2008). Runs consisted of 96 “go” trials in which participants were instructed to indicate whether a horizontal arrow pointed to the left or the right, interspersed with 32 “stop” trials (25% of total trials) in which a red X appeared on top of the arrow, cueing the participant to withhold a respond. Across all trials, arrows were displayed for 1 second, with a 1 second interval, followed by a jittered fixation of 0 to 4 seconds. For the first stop trial of each run, the X appeared .25 seconds after the arrow and remained on the screen for the duration of the arrow stimulus. If the participant correctly stopped on a given stop trial, the time between the appearance of the

arrow and X on the next stop trial increased by .05 seconds; if the participant failed to inhibit a response, the time between the appearance of the arrow and X on the next stop trial decreased by .05 seconds. The duration of the delay between arrow and X was cumulative; time was added to or subtracted from the previous stop trial's duration of delay. Participants completed only one run because of the relatively long task duration (6 min) required to build up a prepotent response.

Analyses

Behavioral analyses.—To evaluate task performance, we selected one accuracy measure and one response time (RT) measure for each task. Variables of interest for the switching task were proportion of correct trials and mean RT for correct trials. Performance measures for the updating task were mean RT for correct trials and hits minus false alarms, or the difference between correct identification of A-back matches and misidentification of non-matches. Performance was collapsed across 1- and 2-back blocks. To correct for positive skew of the hits minus false alarms distribution, we applied a square root transformation. For the inhibition task, performance was evaluated using proportion of correct go trials and stop signal RT (SSRT), which estimates the time it takes to detect and correctly respond to (by inhibiting a response) a stop cue. The SSRT is determined by subtracting the mean time between presentation of the arrow and the red X from the mean RT for go trials.

We applied performance thresholds that corresponded to adequate task comprehension across participants, with the goal of increasing the likelihood that commonalities or differences in task activation accurately reflected the way brain regions are engaged, rather than reflecting individual differences in performance across tasks. Runs were excluded if performance did not meet the following criteria: for the switching task, at least 60% accuracy; for the updating task, at least four correct matches on 1-back blocks, 2 correct matches on 2-back blocks, and no more than 9 false alarms (indicating a match when there is none); for the inhibition task, selecting the correct arrow direction on 70% of trials or more, selecting the wrong direction on fewer than 10% of trials, stop accuracy between 25% and 75%, and stop signal reaction time greater than 50ms (Congdon et al., 2012). Seventy-two runs (12.9% of total collected) were omitted for poor performance. Performance data were averaged across usable runs.

Analyses that included behavioral or demographic data were conducted in *R* version 3.2.3 (R Core Team, 2014). Statistical tests were conducted on standardized values. To account for the nonindependence of data drawn from individuals nested within families, we used the *nlme* R package to run regressions as linear mixed models with random intercepts.

fMRI preprocessing.—Imaging data were preprocessed with the fMRI Expert Analysis Tool in FMRIB Software Library (FSL) version 5.9 (www.fmrib.ox.ac.uk/fsl). High-resolution T_1-weighted structural images underwent skull stripping and brain extraction using Freesurfer version 5.3.0 (Reuter et al., 2010). Functional data were registered to the structural image with a boundary-based algorithm (Greve and Fischl, 2009), and structural images were registered to MNI space with the FMRIB Linear Image Registration Tool (Jenkinson and Smith, 2001). Additional pre-statistics processing included spatial smoothing

using a Gaussian kernel of FWHM 5mm; grand-mean intensity normalization of the 4D dataset by a single multiplicative factor; and high pass temporal filtering (Gaussian-weighted least-squares straight line fitting, with 50s sigma).

First-level analyses for individual task runs were conducted with the FSL's Improved Linear Model, which extends the voxelwise general linear model by estimating and correcting for time series autocorrelation (Woolrich et al., 2001). Data were modeled with a double-gamma HRF convolution. The highpass filter was set at 100s for the switching and inhibition runs and to 200s for the updating runs, the latter representing twice the duration of stimuli presentation. First-level models included six motion regressors; temporal derivatives for each regressor (except for the updating task, due to its block design); a trial-level response time regressor; and nuisance regressors that censored individual volumes identified to have excessive motion, defined as framewise displacement greater than .9mm (Siegel et al., 2014). Two runs (.3% of total collected) were excluded from further analysis due to excessive motion during 60% of frames or more. Of the remaining usable runs, 11.0% of volumes were censored due to movement exceeding .9mm. Thirteen additional runs (2.3% of total collected) did not pass visual inspection at the registration stage and were omitted from subsequent analyses. In total, we retained 195 usable runs across 110 participants for the switching task, 170 usable runs across 100 participants for the updating task, and 100 usable runs across 100 participants for the inhibition task.

EF vs. Baseline Contrasts.—For our primary analyses, we selected contrasts that we anticipated would capture robust EF-related activation for each task. The contrast for the switching task was the *cue period during correct switch trials* (i.e., when participants were cued to focus on a rule that differed from the previous trial) *vs. baseline* (fixation cross during the between-trial jitter and at the end of the run). For the updating task, the contrast was *2-back blocks vs. baseline* (fixation cross following task block). For the inhibition task, the selected contrast was *correct stop trials vs. baseline* (blank screen during the between-trial jitter and at the end of the run).

Second-level analyses, which average contrast estimates over runs for each participant, were carried out by specifying a fixed effects structure within FMRIB Local Analysis of Mixed Effects (FLAME, Beckmann et al., 2003). Third-level group analyses for each task were also executed using FLAME. Statistical maps were thresholded with a cluster-forming threshold of $z > 3.1$ (corresponding to $p < .001$), and whole-brain multiple comparisons were corrected using a cluster-level probability of $p < .05$ generated from Gaussian random field theory. We applied these relatively conservative cluster-based thresholds in line with recent recommendations (Ekland, Nichols, & Knutsson, 2016) and to account for the increased likelihood of identifying false positives at that arises from the nesting of multiple individuals within the same family.

Primary Summed Mask Analysis.: We first aimed to test the extent to which patterns of EF-related activation at the whole-brain level overlapped across tasks. Within the thresholded and familywise error (FWE)-corrected *z*-stat map for each task, we assigned a value of 1 to voxels present in clusters that exhibited significantly greater BOLD activity for the executive condition relative to baseline; voxels that failed to meet this criterion were

assigned a 0. We added the binarized maps for each task together, resulting in a single map displaying voxels from clusters engaged by only one task, across two tasks, and across all three tasks.

Thresholding by Percent of Active Voxels.: In order to probe the stability of the primary results, we conducted an exploratory analysis in which task-overlapping activation was plotted across a range of voxelwise thresholds. Instead of applying cluster-based thresholding using a *z*-stat cutoff, we thresholded the top 15% of activated voxels in the task-specific, FWE-corrected maps. The thresholded maps were then summed as normal. Next, we thresholded the top 14% of activated voxels for each task, then the top 13%, and so on down to the top 1% of activated voxels for each task.

Neuroanatomical ROI Comparison.: Clusters of activation derived from the primary summed mask analysis for the entire sample were compared to the location of 13 adult ROIs based on previous work examining domain-general task-control (i.e., EF) activity (Dosenbach et al., 2006). The coordinates for regions identified in the 2006 paper were refined in a later publication that included more comprehensive and precise functional ROIs (Dosenbach et al., 2010); we used the more recent coordinates to define adult ROIs in the current study. These ROIs, listed along with their coordinates in Supplementary Table 1, included five regions from the cingulo-opercular network and eight regions from the fronto-parietal network. In order to estimate distances between the literature-derived ROIs and the clusters of task-overlapping activity in the child sample, we used the FSL *cluster* tool to identify coordinates for the center of each cluster within the summed mask. The distance between each literature-derived and data- driven ROI was computed as:

$$\text{distance}(mm) = \sqrt{(x_{\text{child}} - x_{\text{adult}})^2 + (y_{\text{child}} - y_{\text{adult}})^2 + (z_{\text{child}} - Z_{\text{adult}})^2}$$

where x, y, and z correspond to the MNI coordinates for the child centers of activity and adult ROIs.

Correlations between Task Activation, Age, and Accuracy.: To address the possibility that overlapping activity across tasks could be driven by within-sample differences in age or performance, we next included mean-centered age as an independent variable in the task-specific GLMs. The resulting maps were binarized and summed, revealing areas of the brain in which age significantly correlated with EF-related activation across the three tasks. We repeated this approach with a separate analysis that incorporated mean-centered accuracy as an independent variable.

Stricter EF Contrasts.—To evaluate the generalizability of our results, we next applied a set of contrasts comparing more demanding task periods to less demanding periods for each task. For the switching task, the selected contrast was *correct switch trials vs. correct repeat trials* during the cue period. For the updating task, the contrast was *2-back blocks vs. 1-back blocks.* For the inhibition task, the contrast was *correct stop trials vs. correct go trials*. Because of the more constrained nature of these contrasts, relative to contrasts including

baseline, the cluster- forming threshold was lowered to $z > 2.3$, and the cluster-correction threshold was raised to $p < .01$.

Response Time vs. Baseline Contrasts.—To compare time-on-task effects to the results of the principal analyses, we applied *response time vs. baseline* contrasts to the switching and inhibition tasks. Modeling trial-by-trial RT as a regressor in the GLM for each task not only decreases the likelihood that activation observed for other conditions of interest is confounded by corresponding fluctuations in RT, but also can be leveraged to identify brain areas whose activation corresponds to RT differences (Yarkoni et al., 2009). The updating task could not be incorporated into this analysis due to the nature of the block design. The thresholded ($z > 3.1$) and FWE-corrected ($p < .05$) *response time vs. baseline* maps for the switching and inhibition tasks were binarized and summed to identify brain areas whose activation corresponded to variation in RT.

Subsample Analyses.—Applying the *EF vs. baseline* contrasts described earlier, we conducted a group comparison to evaluate activation differences across younger (≤ 10.5 years, $N = 62$) and older (> 10.5 years, $N = 55$) subgroups. Activation differences for males ($N = 60$) and females ($N = 57$) were also investigated. We next looked at cross-task EF activation within a subsample of individuals free of learning or developmental disorder diagnoses ($N = 109$). In a final analysis, cross-task activation was evaluated for a subsample of unrelated individuals, addressing the possibility that task-overlapping activity could be attributed to the sampling of multiple individuals from the same family. This analysis included one twin from each pair and half of the unpaired individuals (total $N = 58$). The analyzed and un-analyzed sample halves were matched on age, sex, IQ, and number of usable tasks.

Results

Task Performance

Descriptive statistics for task performance are provided in Table 1. As expected, performance covaried across tasks: The average zero-order correlation for accuracy between any two of the three tasks was .46; the average zero-order correlation for response time was .24. We report standardized regression coefficients from mixed models that included participant family as a random effect and performance, age, and sex as fixed effects. Performance relations with age are depicted in Supplementary Figure 2a. Age was significantly associated with switching accuracy ($ß = .43$, $SE = .10$, $p < .001$), updating hits minus false alarms ($ß = .25$, $SE = .10$, $p < .05$), and updating response time ($ß = -.25$, $SE = .10$, $p < .05$). Age did not significantly predict switching response time ($ß = -.16$, $SE = .11$, $p = .13$), inhibition accuracy ($ß = .16$, $SE = .11$, $p = .15$), or inhibition response time ($ß = -.19$, $SE = .11$, $p = .09$). Performance relations with sex are depicted in Supplementary Figure 2b. Task performance differed by sex for updating response time, such that males responded .07s more quickly than females on average ($ß = -.23$, $SE = .10$, $p < .05$). Inhibition response time also significantly differed by sex, such that females' stop signal RTs were, on average, .02s faster than males' ($ß = .21$, $SE = .10$, $p < .05$).

Neuroimaging Results: Full Sample

EF vs. Baseline Contrasts.—The results of the task-specific analyses are shown in Figure 1. Cluster information for these maps is provided in Supplementary Tables 2–4.

Summed Mask Results.: To examine the extent to which EF-related activity overlapped across tasks at the group level, we binarized the thresholded and cluster-corrected positive *z*-stat map for each task, then added the maps together to visualize areas of activation common across the three tasks (Figure 2). Significant task-positive activity common across all three EF domains was observed in the dorsal anterior cingulate cortex (dACC), bilateral anterior insula, right dorsolateral prefrontal cortex (dlPFC), right middle frontal gyrus (MFG), bilateral frontal eye fields (FEF), bilateral superior parietal lobule (SPL), and bilateral inferior parietal lobule (IPL). Table 2 provides details on these regions, including center of gravity coordinates and cluster sizes from FSL's *cluster* tool.

Thresholding by Percent of Active Voxels.: We next applied the summed mask approach to task-specific maps thresholded on the basis of the top 15% of activated voxels, down to the top 1% of activated voxels. The summed masks from this exploratory analysis are shown in a video graphic available at https://youtu.be/2pgE74MDW8I [temporary link]. The top voxel activity results were highly consistent with the cluster-based result, demonstrating a preservation across thresholds of overlapping activity in areas consistent with adult control regions. Even when only the top 1% of active voxels for each task were included in the summed mask, there were large areas of overlap centered upon bilateral insula, dACC, and bilateral SPL.

Neuroanatomical ROI Comparison.: Our primary aim with respect to the adult literature-derived ROIs was determining whether they converged with clusters exhibiting cross-task activity in our developmental sample. Figure 2 displays the literature-derived ROIs in pink, overlaid on activity common across two or more of the EF tasks at the original cluster-based thresholds. Ten of the 13 ROIs fell within areas of task-overlapping activity. Adult ROIs that fell within or bordered activity common across all tasks were bilateral anterior insula, dACC, bilateral inferior parietal sulcus (IPS), right frontal, right dlPFC, and right IPL. The left dlPFC and left frontal ROIs from the adult literature fell within a cluster of activity common across the switching and updating contrasts. Neither of the bilateral anterior prefrontal cortex ROIs nor the left IPL ROI converged with cross-task activity at the designated cluster thresholds.

To quantitatively compare the location of adult ROIs to children's task-common activity, we computed the distance between the 13 a priori ROIs and the centers of 11 clusters of activity from our child sample. The majority of centroids representing overlapping activity in our child sample were within 15mm of the adult-based ROIs (see Supplementary Table 5). Specifically, child activation in dACC, bilateral anterior insula, right MFG, right IPL, and left SPL lay 10mm or less from corresponding adult regions. Child activation in right dlPFC, left IPL, and right SPL were 10–14mm from corresponding adult regions. The regions derived from the child data that were more distal from adult ROIs were bilateral FEF, each approximately 25mm from the adult frontal ROIs.

Age & Accuracy Correlations.: To determine whether age differences within the sample accounted for overlapping activation across EF tasks, we included mean-centered age as an independent variable in the GLM for each task. Age negatively correlated with BOLD activity during the updating task in right ventral striatum (cluster peak coordinates: 8, 16, −10; 231 voxels) and left ventromedial PFC (−10, 30, −6; 107 voxels). There were no significant clusters of age-correlated activity shared by the three tasks.

Accuracy positively correlated with BOLD activity during the switching task in right lingual gyrus (12, −78, −10; 96 voxels) and during the inhibition task in right anterior insula (42, 24, −4; 130 voxels). Updating accuracy negatively correlated with activation during the updating task in left ventral striatum (−6, 14, −8; 121 voxels). There were no significant clusters of accuracy-correlated activity shared by the three tasks.

Stricter EF Contrasts.—We conducted a summed-mask analysis using the following contrasts for the switching, updating, and inhibition domains, respectively: *correct switch trials vs. correct repeat trials during the cue period, 2-back block vs. 1-back block, stop trials vs. correct go trials.* As displayed in Figure 3 and detailed in Table 3, significant activity shared across all tasks was observed in small clusters within dACC, right anterior insula, right FEF, left inferior frontal sulcus, and left IPL. The center of dACC activation was 7mm from the corresponding adult dACC region. Activation in the right insula, left inferior frontal sulcus, and left IPL were 8, 12, and 19mm, respectively, from the right insula, left frontal, and left IPL adult ROIs. Right FEF activity was greater than 20mm from any adult region. At a more stringent cluster-forming threshold of $z > 3.1$, there were no significant clusters common across the three tasks.

Response Time vs. Baseline Contrasts.—We next applied the summed-mask approach to the *response time vs. baseline* contrasts for the switching and inhibition tasks. Clusters of significant activity corresponding to trial-by-trial response time across tasks were observed in dACC, right primary motor cortex, right superior frontal gyrus, and right thalamus (Figure 4, Table 4).

Neuroimaging Results: Subsamples

Group Comparisons: Age and Sex.—To evaluate age-related differences in EF activity, we conducted a group comparison between younger and older subsamples split at age 10.5 years. There were no regions for which *EF vs. baseline* activation differed across the age groups in all three tasks. We conducted an additional group comparison to identify EF-related activation differences between males and females. As in the age-group analysis, there were no areas that showed sex differences across the three tasks. Task-specific results for the group comparisons are depicted in Supplementary Figure 3.

Comparison of Full Sample to Undiagnosed Participants and Unrelated Participants.—Supplementary Figure 4a depicts task-unique and task-common activity for the full sample. After excluding eight participants diagnosed with developmental and/or learning disorders, the centers and spread of activation were nearly identical to those of the full sample (Supplementary Figure 4b, Supplementary Table 6). To determine whether the

robustness of our primary results was driven by the inclusion of multiple individuals from the same family, we repeated the analysis with a subsample of unrelated individuals. As depicted in Supplementary Figure 4c and detailed in Supplementary Table 6, the task-overlapping map from the analysis of unrelated individuals was consistent with that of the full sample.

Discussion

Executive functions are foundational processes that underlie the development of complex reasoning and mediate environmental risk for negative outcomes (Best et al., 2011; Nesbitt et al., 2013; Zelazo and Müller, 2002). Understanding the neurobiological organization of EFs as they undergo rapid maturation in childhood is key to developing interventions that promote EF development, ameliorate executive deficits, and identify risk factors for impending cognitive and psychiatric impairments. An outstanding question is whether the functional brain networks that support domain-general EFs in adulthood are in place by middle childhood or whether they are substantively different. Motivated by well documented findings of task-overlapping activity in the adult literature (Crittenden et al., 2016; Dosenbach et al., 2006), meta-analyses of single-task studies of children's EF-related activation (Houdé et al., 2010; McKenna et al., 2017), and behavioral studies showing consistency in the factor structure of EF performance across development, we examined brain activation across three EF domains in a single, population- representative sample of children. This approach provided an opportunity to make inferences about task-general EF processing that past approaches have not been capable of.

Activity Shared Across EFs in Childhood Centers upon Fronto-parietal and Cingulo-opercular Regions

We found that children engaged a common set of brain regions across EF domains. The largest clusters of cross-task activation were observed in dACC, bilateral anterior insula, and bilateral SPL. Additional overlap occurred in right posterior MFG, right dlPFC, bilateral FEF, and bilateral supramarginal gyri of the IPL. Regions of co-activation in this sample of children and early adolescents were consistent with the two EF networks that have been well characterized in adults. Specifically, regions comprising the adult cingulo-opercular network (dACC, bilateral anterior insula) and the fronto-parietal network (right dlPFC, bilateral MFG, bilateral SPL, bilateral IPL) co-activated in response to EF demands in our sample. Additionally, bilateral frontal eye fields at the intersection of the middle frontal and precentral gyri exhibited significant activation across all three tasks. Although FEFs are absent from task-related EF networks in studies of adults, these regions are functionally correlated to regions in the adult fronto-parietal network during resting state (Cole et al., 2013; Fox et al., 2005; Gordon et al., 2016; Grinband et al., 2008; Power et al., 2011; Yeo et al., 2011). Our findings indicate that established patterns of neural activity underlying adult EFs are qualitatively similar to those observed in middle childhood. Thus, the development of EFs from middle childhood to adulthood likely involves quantitative changes in activity within EF-related networks, rather than qualitative changes in the organization of the networks themselves.

Employing stricter contrasts for the tasks revealed a specialized set of regions that were engaged across more demanding task periods. Clusters were centered upon dACC and right anterior insula, as well as right FEF, left IFS, and left IPL. In adults, the dACC and anterior insula have been found to constitute a "core task-set system" based on their involvement across distinct trial periods and executive domains (Dosenbach et al., 2006; Menon and Uddin, 2010). Dosenbach and colleagues (2006) identified these as the only regions whose activity overlapped when combining thresholded ROI maps representing initiation of cognitively demanding tasks, maintenance of task rules, and performance-related feedback. A recent meta-analysis that examined children's BOLD signal responses to solving mathematical problems also reported robust activation of the right insula across task contexts (Arsalidou, Pawliw-Levac, Sadeghi, & Pascual-Leone, 2018). As the insula is not traditionally included in neural models of mathematical problem solving, the authors interpreted this finding as evidence that the insula, in conjunction with the dACC, is involved in motivated behaviors. Considered together, the current results and those of previous meta-analyses support the proposition that, in both childhood and adulthood, co-activation of cingulo-opercular regions is necessary for the execution of highly demanding tasks. Overall, the results of the primary and sensitivity analyses imply that well documented increases in EF abilities from middle childhood to adulthood operate via a stable and common functional architecture, though a comparison of child and adult groups or a longitudinal investigation of the same individuals over time is necessary to test this directly.

Importantly, our key findings were independent of commonalities driven by response time, as trial-by-trial RT was included as a regressor in first-level analyses. This was a critical advantage of the current study, as meta-analyses of the neural basis of EFs in childhood are unable to dissociate activation attributable to executive processes per se from activation attributable to response time. The importance of this step was underscored by our finding that within-person differences in RT corresponded to cross-task activity in a region consistently linked to executive processing, the dACC. RT-related activation in this region and primary motor cortex is consistent with RT effects observed in adult samples (Grinband et al., 2008; Yarkoni et al., 2009), though many clusters of task-overlapping activity remained unique to the EF contrasts. In summary, we found that activity in a region critical to EF, the dACC, related to a standard behavioral outcome, but that activity in these regions also occurred above and beyond performance differences across individuals.

Commonalities in children's brain activation across switching, updating, and inhibition tasks may serve as the neural corollary for behavioral evidence that individual differences in EF task performance are best captured by a hierarchical model in which variance is shared across domain-specific EF factors, suggesting that common causal processes act on individual EFs (Engelhardt et al., 2015; Miyake et al., 2000). Indeed, variance shared across EF domains is attributable primarily to genetic factors; a general factor of EF has been found to be nearly 100% heritable in samples of 7- to 14-year-olds (Engelhardt et al., 2015) and young adults (Friedman et al., 2008), with negligible contributions from environmental sources. Executive function thus constitutes one of the most genetically influenced phenotypes early in life, and our finding that the neural architecture of EFs is effectively in place when the heritability of EF is at its peak may help to clarify the pathways by which genetic variation leads to individual differences in abilities supported by EF.

Implications for Future Research

The convergence of our results across brain activity and behavioral models clearly suggests that the organizational foundation for EFs is in place by middle childhood. The question that logically follows is: What mechanisms underlie the large gains in executive skills from middle childhood forward? One possibility is that changes in EF performance result from functional changes in the task-common regions we have described. For example, strength of co-activation between pairs or subsets of regions may increase with repeated engagement in EF- demanding situations over development (Johnson, 2011). In a study of typical development of intrinsic functional connectivity of the default mode network, Chai and colleagues (2014) demonstrated that resting-state connectivity between default regions and many of the EF-relevant regions highlighted in the current study becomes more negative from childhood to adulthood. The authors suggest that the development of these intrinsic correlations underlies age-related improvements in EF abilities. In the current study, we focused on global patterns of activation rather than inter-regional relatedness, but examining finer-tuned synchronicity between regions that exhibited significant activation across our tasks will likely prove fruitful.

Another possibility is that structural maturation of brain regions and their connections mediates behavioral improvement in EFs. Exploring this possibility, Baum and colleagues (2017) examined age-related changes in white matter-based connectivity and EF abilities in a cross-sectional sample of children through young adults. The degree to which white matter connectivity was stronger within functional modules (e.g., somatosensory regions, fronto-parietal regions) mediated developmental increases in performance on an EF task. The integration of functional and structural neuroimaging approaches would shed light on the mechanisms by which various neural properties interact to support the development of EFs.

Other extensions of this work may focus on the role of cingulo-opercular and frontoparietal regions in the onset and maintenance of atypical thoughts and behaviors, as EF deficits have been implicated in nearly every developmental disorder (Carlson et al., 2013; Zelazo and Müller, 2002). The current results could provide a baseline against which studies of atypical development may be compared. For example, the regions highlighted in the current paper (in particular, dACC and bilateral anterior insula) show robust activation in the face of different executive demands. Hypo- or hyperactivation of these regions may therefore correspond to poor EF performance, as well as symptom burden. A recent meta-analysis of adult neuroimaging studies examined brain activity in response to EF tasks, comparing healthy controls to participants with various psychiatric disorders (McTeague et al., 2017). Regardless of disorder type, EF-related activity among diagnosed groups consistently differed from that of healthy controls in left anterior insula, right ventrolateral PFC, right IPS, right motor regions, and anterior dACC. The authors proposed that brain networks that support adaptive cognitive control, like the fronto-parietal network, are especially vulnerable to disruptions that may manifest as psychopathology. Alternatively, divergence from established EF-related regions may be symptomatic of psychiatric or developmental disorders (Menon, 2011).

The current results tell us about developmental norms with respect to children’s functional brain organization. Future research that looks beyond group means may lead to greater

understanding of the practical consequences and correlates of individual differences in engaging regions common across or unique to EF domains. For example, it may be that the regions we have identified here are required for successfully engaging in a task, whereas task-unique activation exhibits greater variability that may meaningfully relate to differences in age-varying task performance or other behavioral outcomes (Braver et al., 2010; Yarkoni and Braver, 2010). In our primary analyses, contrasts for the event-related tasks (switching and inhibition) included correct trials alone, as a means of targeting successful engagement of EFs. More extensive associations between BOLD activity and task performance may be detected with contrasts that combine across correct and incorrect trials.

Limitations

We acknowledge a number of limitations in the current study, including a lack of collection of the same set of tasks in adults. However, adult EF activity has been well established across multiple tasks within large samples (e.g., Crittenden et al., 2016; Dosenbach et al., 2006). By capitalizing on extant adult datasets, we were able to estimate the spatial proximity of hubs of activity in our sample to that of well characterized adult ROIs. The idiosyncrasies inherent to the tasks we selected constitute another limitation. In particular, the inhibition task led to strongly right-lateralized activation, potentially explaining the fewer left hemisphere overlaps across all three tasks. However, our tasks benefited from strong performance in the current sample, which is critical when interpreting developmentally normative brain activation during tasks, as error- related BOLD responses can differ systematically from more task-relevant signals (Church et al., 2010; Murphy and Garavan, 2004).

Another potential limitation involves the mapping of children's structural scans into a stereotactic space derived from scans of young adults. Reports of misclassification of children's brain tissue when normalizing structural images to a common stereotactic space have led to concerns that age-related structural differences generate spurious age-related differences in brain activation (Richards & Wie, 2015). It is possible, for example, that inconsistencies between locations of children and adult task-overlapping activation are driven by age-related structural differences. However, a separate body of empirical work has demonstrated that, after transforming images into a common stereotactic space, differences between children as young as 7 years of age and adults in the location and variability of anatomical structures are minor, especially relative to the spatial resolution of group fMRI images (Bergund et al., 2002). Furthermore, such differences are unlikely to produce spurious differences in functional activation (Kang et al., 2003).

Conclusion

The goal of this study was to evaluate the consistency of children's brain activation in response to various EF demands and to determine whether co-activated regions followed the organization observed among adults. The study benefited from a large, representative sample measured on multiple tasks, conferring greater precision than that afforded by meta-analyses. The results indicated that, by middle childhood, a common set of fronto-parietal and cingulo- opercular regions support executive processing across EF domains. The results shed light on the neurobiological bases of a set of abilities that are critical for everyday

functioning and lifelong wellbeing, indicating the organization is established by middle childhood. Further exploration of correlates of task overlapping and task unique EF-related signals presents an exciting opportunity to understand cognitive maturation in typical and atypical development.

Supplementary Material

Refer to Web version on PubMed Central for supplementary material.

Acknowledgements

This project was supported by National Institutes of Health grants R21 HD081437 (ETD and JAC) and R01 HD083613 (ETD), as well as University of Texas Imaging Research Center pilot grant 20141031a (LEE). L. E. Engelhardt was supported by a National Science Foundation Graduate Research Fellowship. K. P. Harden and E. M. Tucker-Drob are each supported by Jacobs Foundation Research Fellowships. The Population Research Center at the University of Texas at Austin is supported by National Institutes grant R24 HD042849. We wish to thank the research team that facilitated data collection: Mary Abbe Roe, Jessica Graves, Annie Zheng, Damion Demeter, Saloni Kumar, Mackenzie Mitchell, and Tehila Nugiel. Finally, we thank our participating families for their time and effort.

References

Aron AR, 2008 Progress in executive-function research: From tasks to functions to regions to networks. Curr. Dir. Psychol. Sci. 17, 124–129. doi.org/10.1111/j.1467-8721.2008.00561.x

Arsalidou M, Pawliw-Levac M, Sadeghi M, Pascual-Leone J, 2018 Brain areas associated with numbers and calculations in children: Meta-analyses of fMRI studies. Dev. Cogn. Neurosci. 30, 239–250. doi.org/10.1016/j.dcn.2017.08.002 [PubMed: 28844728]

Banich MT, 2009 Executive function: The search for an integrated account. Curr. Dir. Psychol. Sci. 18, 89–94.

Baum GL, Ciric R, Roalf DR, Betzel RF, Moore TM, Shinohara RT, Kahn AE, Vandekar SN, Rupert PE, Quarmley M, Cook PA, Elliott MA, Ruparel K, Gur RE, Gur RC, Bassett DS, Satterthwaite TD, 2017 Modular segregation of structural brain networks supports the development of executive function in youth. Curr. Biol. 27, 1561–1572. doi.org/10.1016/j.cub.2017.04.051 [PubMed: 28552358]

Baym CL, Corbett BA, Wright SB, Bunge SA, 2008 Neural correlates of tic severity and cognitive control in children with Tourette syndrome. Brain 131, 165–179. doi. org/10.1093/brain/awm278 [PubMed: 18056159]

Beckmann C, Jenkinson M, Smith SM, 2003 General multi-level linear modelling for group analysis in FMRI. Neuroimage 20, 1052–1063. doi.org/10.1016/S1053-8119(03)00435-X [PubMed: 14568475]

Best JR, Miller PH, 2010 A developmental perspective on executive function. Child Dev. 81, 1641–1660. doi.org/10.1111/j.1467-8624.2010.01499.x [PubMed: 21077853]

Best JR, Miller PH, Naglieri JA, 2011 Relations between executive function and academic achievement from ages 5 to 17 in a large, representative national sample. Learn. Individ. Differ. 21, 327–336. [PubMed: 21845021]

Braver TS, Cole MW, Yarkoni T, 2010 Vive les differences! Individual variation in neural mechanisms of executive control. Curr. Opin. Neurobiol. doi.org/10.1016/j.conb.2010.03.002

Buckner RL, 2004 Memory and executive function in aging and AD: Multiple factors that cause decline and reserve factors that compensate. Neuron. doi. org/10.1016/j.neuron.2004.09.006

Bunge SA, Wright SB, 2007 Neurodevelopmental changes in working memory and cognitive control. Curr. Opin. Neurobiol. 17, 243–250. doi.org/10.1016/j.conb.2007.02.005 [PubMed: 17321127]

Burgund ED, Kang HC, Kelly JE, Buckner RL, Snyder AZ, Petersen SE, Schlaggar BL, 2002 The feasibility of a common stereotactic space for children and adults in fMRI studies of development. Neuroimage 17, 184–200. [PubMed: 12482076]

Cacioppo JT, Petty RE, Feng Kao C, 1984 The efficient assessment of need for cognition. J. Pers. Assess. 48, 306–307. [PubMed: 16367530]

Carlson SM, Zelazo PD, Faja S, 2013 Executive function, in: Zelazo PD (Ed.), Oxford Handbook of Developmental Psychology. Oxford University Press, New York, pp. 706–742.

Chai XJ, Ofen N, Gabrieli JD and Whitfield-Gabrieli S, Selective development of anticorrelated networks in the intrinsic functional organization of the human brain, J. Cogn. Neurosci. 26, 2014, 501–513. [PubMed: 24188367]

Church JA, Bunge SA, Petersen SE, Schlaggar BL, 2017 Preparatory engagement of cognitive control networks increases late in childhood. Cereb. Cortex 27, 2139–2153. doi. org/10.1093/cercor/bhw046 [PubMed: 26972753]

Church JA, Petersen SE, Schlaggar BL, 2010 The "Task B problem" and other considerations in developmental functional neuroimaging. Hum. Brain Mapp. 31, 852–862. doi. org/10.1002/hbm.21036 [PubMed: 20496376]

Cole MW, Reynolds JR, Power JD, Repovs G, Anticevic A, Braver TS, 2013 Multi-task connectivity reveals flexible hubs for adaptive task control. Nat. Neurosci. 16, 1348–1355. [PubMed: 23892552]

Collette F, Hogge M, Salmon E, Van der Linden M, 2006 Exploration of the neural substrates of executive functioning by functional neuroimaging. Neuroscience 139, 209–221. doi.org/10.1016/j.neuroscience.2005.05.035 [PubMed: 16324796]

Congdon E, Mumford JA, Cohen JR, Galvan A, Aron AR, Xue G, Miller E, Poldrack RA, 2010 Engagement of large-scale networks is related to individual differences in inhibitory control. Neuroimage 53, 653–663. [PubMed: 20600962]

Congdon E, Mumford JA, Cohen JR, Galvan A, Canli T, Poldrack RA, 2012 Measurement and reliability of response inhibition. Front. Psychol. 3. doi. org/10.3389/fpsyg.2012.00037

Crittenden BM, Mitchell DJ, Duncan J, 2016 Task encoding across the multiple demand cortex is consistent with a frontoparietal and cingulo-opercular dual networks distinction. J. Neurosci. 36, 6147–6155. doi.org/10.1523/jneurosci.4590-15.2016 [PubMed: 27277793]

Crone EA, Dahl RE, 2012 Understanding adolescence as a period of social-affective engagement and goal flexibility. Nat. Rev. Neurosci. 13, 636–650. doi.org/10.1038/nrn3313 [PubMed: 22903221]

Diamond A, 2002 Normal development of prefrontal cortex from birth to young adulthood: Cognitive functions, anatomy, and biochemistry, in: Stuss DT, Knight RT (Eds.), Principles of Frontal Lobe Function. Oxford University Press, New York, pp. 466–503. doi.org/10.1093/acprof:oso/9780195134971.003.0029

Dosenbach NU, Visscher KM, Palmer ED, Miezin FM, Wenger KK, Kang HC, Burgund ED, Grimes AL, Schlaggar BL, Petersen SE, 2006 A core system for the implementation of task sets. Neuron 50, 799–812. doi.org/10.1016/j.neuron.2006.04.031 [PubMed: 16731517]

Dosenbach NUF, Fair DA, Cohen AL, Schlaggar BL, Petersen SE, 2008 A dual-networks architecture of top-down control. Trends Cogn. Sci. 12, 99–105. [PubMed: 18262825]

Dosenbach NUF, Fair DA, Miezin FM, Cohen AL, Wenger KK, Dosenbach RAT, Fox MD, Snyder AZ, Vincent JL, Raichle ME, 2007 Distinct brain networks for adaptive and stable task control in humans. Proc. Natl. Acad. Sci. 104, 11073–11078. [PubMed: 17576922]

Dosenbach NUF, Nardos B, Cohen AL, Fair DA, Power D, Church JA, Nelson SM, Wig GS, Vogel AC, Lessov-schlaggar CN, Barnes KA, Dubis JW, Feczko E, Coalson RS, Priett JR, Barch DM, Petersen SE, Schlaggar BL, 2010 Prediction of individual brain maturity using fMRI. Science. 329, 1358–1361. doi.org/10.1126/science.1194144. [PubMed: 20829489]

Eklund A, Nichols TE, Knutsson H, 2016). Cluster failure: Why fMRI inferences for spatial extent have inflated false-positive rates. Proc. Natl. Acad. Sci. 113, 7900–7905. [PubMed: 27357684]

Engelhardt LE, Briley DA, Mann FD, Harden KP, Tucker-Drob EM, 2015 Genes unite executive functions in childhood. Psychol. Sci. 26, 1151–1163. [PubMed: 26246520]

Fox MD, Snyder AZ, Vincent JL, Corbetta M, Van Essen DC, Raichle ME, Corbetta M, 2005 The human brain is intrinsically organized into dynamic, anticorrelated functional networks. Proc. Natl. Acad. Sci. 102, 9673–9678. [PubMed: 15976020]

Friedman NP, Miyake A, Young SE, Defries JC, Corley RP, Hewitt JK, 2008 Individual differences in executive functions are almost entirely genetic in origin. J. Exp. Psychol. Gen. 137, 201–225. [PubMed: 18473654]

Gordon EM, Laumann TO, Adeyemo B, Huckins JF, Kelley WM, Petersen SE, 2016 Generation and evaluation of a cortical area parcellation from resting-state correlations. Cereb. Cortex 26, 288–303. [PubMed: 25316338]

Greve DN, Fischl B, 2009 Accurate and robust brain image alignment using boundary-based registration. Neuroimage 48, 63–72. doi.org/10.1016/j.neuroimage.2009.06.060 [PubMed: 19573611]

Grinband J, Wager TD, Lindquist M, Ferrera VP, Hirsch J, 2008 Detection of time- varying signals in event-related fMRI designs. Neuroimage 43, 509–520. doi.org/10.1016/j.neuroimage.2008.07.065 [PubMed: 18775784]

Harden KP, Tucker-Drob EM, Tackett JL, 2013 The Texas Twin Project. Twin Res. Hum. Genet. 16, 385–390. [PubMed: 23111007]

Houdé O, Rossi S, Lubin A, Joliot M, 2010 Mapping numerical processing, reading, and executive functions in the developing brain: an fMRI meta-analysis of 52 studies including 842 children. Dev. Sci. 13, 876–885. doi.org/10.1111/j.1467-7687.2009.00938.x [PubMed: 20977558]

Huizinga M, Dolan CV, van der Molen MW, 2006 Age-related change in executive function: Developmental trends and a latent variable analysis. Neuropsychologia 44, 2017–2036. [PubMed: 16527316]

Jaeggi SM, Studer-Luethi B, Buschkuehl M, Su Y-F, Jonides J, Perrig WJ, 2010 The relationship between n-back performance and matrix reasoning — implications for training and transfer. Intelligence 38, 625–635.

Jenkinson M, Smith S, 2001 A global optimisation method for robust affine registration of brain images. Med. Image Anal. 5, 143–156. doi.org/10.1016/S1361-8415(01)00036-6 [PubMed: 11516708]

Johnson MH, 2011 Interactive specialization: A domain-general framework for human functional brain development? Dev. Cogn. Neurosci. 1, 7–21. [PubMed: 22436416]

Johnson MH, 2001 Functional brain development in humans. Nat. Rev. Neurosci. 2, 475–483. doi.org/10.1038/35081509 [PubMed: 11433372]

Johnson MH, 1990 Cortical maturation and the development of visual attention in early infancy. J. Cogn. Neurosci. 2, 81–95. doi.org/10.1162/jocn.1990.2.2.81 [PubMed: 23972019]

Kang HC, Burgund ED, Lugar HM, Petersen SE, Schlaggar BL, 2003 Comparison of functional activation foci in children and adults using a common stereotactic space. Neuroimage 19, 16–28. doi.org/10.1016/s1053-8119(03)00038-7 [PubMed: 12781724]

Luna B, Garver KE, Urban TA, Lazar NA, Sweeney JA, 2004 Maturation of cognitive processes from late childhood to adulthood. Child Dev. 75, 1357–1372. doi.org/10.1111/j.1467-8624.2004.00745.x [PubMed: 15369519]

McKenna R, Rushe T, Woodcock KA, 2017 Informing the structure of executive function in children: A meta-analysis of functional neuroimaging data. Front. Hum. Neurosci. 11, 1–17. doi. org/10.3389/fnhum.2017.00154 [PubMed: 28149275]

McTeague LM, Huemer J, Carreon DM, Jiang Y, Eickhoff SB, Etkin A, 2017 Identification of common neural circuit disruptions in cognitive control across psychiatric disorders. Am. J. Psychiatry 174, 676–685. doi.org/10.1176/appi.ajp.2017.16040400 [PubMed: 28320224]

Menon V, 2011 Large-scale brain networks and psychopathology: A unifying triple network model. Trends Cogn. Sci. 15, 483–506. doi.org/10.1016/j.tics.2011.08.003 [PubMed: 21908230]

Menon V, Uddin LQ, 2010 Saliency, switching, attention and control: A network model of insula function. Brain Struct. Funct. 214, 655–667. doi.org/10.1007/s00429-010-0262-0 [PubMed: 20512370]

Miyake A, Friedman NP, Emerson MJ, Witzki AH, Howerter A, Wager TD, 2000 The unity and diversity of executive functions and their contributions to complex “frontal lobe” tasks: A latent variable analysis. Cogn. Psychol. 41, 49–100. [PubMed: 10945922]

Murphy K, Garavan H, 2004 Artifactual fMRI group and condition differences driven by performance confounds. Neuroimage 21, 219–228. doi. org/10.1016/j.neuroimage.2003.09.016 [PubMed: 14741659]

Nee DE, Brown JW, Askren MK, Berman MG, Demiralp E, Krawitz A, Jonides J, 2012 A meta-analysis of executive components of working memory. Cereb. Cortex 23, 264–282. doi.org/10.1093/cercor/bhs007 [PubMed: 22314046]

Nesbitt KT, Baker-Ward L, Willoughby MT, 2013 Executive function mediates socio-economic and racial differences in early academic achievement. Early Child. Res. Q. 28, 774–783. doi.org/10.1016/j.ecresq.2013.07.005

Niendam TA, Laird AR, Ray KL, Dean YM, Glahn DC, Carter CS, 2012 Meta- analytic evidence for a superordinate cognitive control network subserving diverse executive functions. Cogn. Affect. Behav. Neurosci. 12, 241–268. doi.org/10.3758/s13415-011-0083-5 [PubMed: 22282036]

Ofen N, Kao Y-C, Sokol-Hessner P, Kim H, Whitfield-Gabrieli S, Gabrieli JDE, 2007 Development of the declarative memory system in the human brain. Nat. Neurosci. 10, 1198–1205. doi.org/10.1038/nn1950 [PubMed: 17676059]

Ollinger JM, Shulman GL, Corbetta M, 2001 Separating processes within a trial in event- related functional MRI, I. The method. Neuroimage 13, 210–217. doi.org/10.1006/nimg.2000.0710 [PubMed: 11133323]

Ordaz SJ, Foran W, Velanova K, Luna B, 2013 Longitudinal growth curves of brain function underlying inhibitory control through adolescence. J. Neurosci. 33, 18109–18124. doi.org/10.1523/jneurosci.1741-13.2013 [PubMed: 24227721]

Owen AM, McMillan KM, Laird AR, Bullmore E, 2005 N-back working memory paradigm: A meta-analysis of normative functional neuroimaging studies. Hum. Brain Mapp. 25, 46–59. [PubMed: 15846822]

Peirce JW, 2007 PsychoPy - Psychophysics software in Python. J. Neurosci. Methods 162, 8–13. doi.org/10.1016/j.jneumeth.2006.11.017 [PubMed: 17254636]

Power JD, Barnes KA, Snyder AZ, Schlaggar BL, Petersen SE, 2012 Spurious but systematic correlations in functional connectivity MRI networks arise from subject motion. Neuroimage 59, 2142–2154. doi.org/10.1016/j.neuroimage.2011.10.018 [PubMed: 22019881]

Power JD, Cohen AL, Nelson SM, Wig GS, Barnes KA, Church JA, Vogel AC, Laumann TO, Miezin FM, Schlaggar BL, Petersen SE, 2011 Functional network organization of the human brain. Neuron 72, 665–678. doi.org/10.1016/j.neuron.2011.09.006 [PubMed: 22099467]

R Core Team, 2014. R: A language and environment for statistical computing.

Reuter M, Rosas HD, Fischl B, 2010 Highly accurate inverse consistent registration: A robust approach. Neuroimage 53, 1181–1196. doi.org/10.1016/j.neuroimage.2010.07.020 [PubMed: 20637289]

Richards JE, Xie W, 2015 Chapter one - Brains for all the ages: Structural neurodevelopment in infants and children from a life-span perspective. Adv Child Dev Behav 48, 1–52. [PubMed: 25735940]

Rueda MR, Fan J, McCandliss BD, Halparin JD, Gruber DB, Lercari LP, Posner MI, 2004 Development of attentional networks in childhood. Neuropsychologia 42, 1029–1040. doi. org/10.1016/j.neuropsychologia.2003.12.012 [PubMed: 15093142]

Salthouse TA, Atkinson TM, Berish DE, 2003 Executive functioning as a potential mediator of age-related cognitive decline in normal adults. J. Exp. Psychol. Gen. 132, 566–594. doi.org/10.1037/0096-3445.132.4.566 [PubMed: 14640849]

Siegel JS, Power JD, Dubis JW, Vogel AC, Church JA, Schlaggar BL, Petersen SE, 2014 Statistical improvements in functional magnetic resonance imaging analyses produced by censoring high-motion data points. Hum. Brain Mapp. 35, 1981–1996. doi.org/10.1002/hbm.22307 [PubMed: 23861343]

Thelen E, 1995 Motor development: A new synthesis. Am. Psychol. doi.org/10.1037/0003-066X.50.2.79

Tucker-Drob EM, 2011 Individual differences methods for randomized experiments. Psychol. Methods 16, 298–318. doi.org/10.1037/a0023349 [PubMed: 21744970]

Verbruggen F, Logan GD, 2008 Response inhibition in the stop-signal paradigm. Trends Cogn. Sci. 12, 418–424. doi.org/10.1016/j.tics.2008.07.005 [PubMed: 18799345]

Woolrich MW, Ripley BD, Brady M, Smith SM, 2001 Temporal autocorrelation in univariate linear modeling of FMRI data. Neuroimage 14, 1370–1386. doi.org/10.1006/nimg.2001.0931 [PubMed: 11707093]

Yaple Z, Arsalidou M, 2018 *N*-back working memory task: Meta-analysis of normative fMRI studies with children. Child Dev. doi.org/10.1111/cdev.13080

Yarkoni T, Barch DM, Gray JR, Conturo TE, Braver TS, 2009 BOLD correlates of trial-by-trial reaction time variability in gray and white matter: A multi-study fMRI analysis. PLoS One 4, e4257. doi.org/10.1371/journal.pone.0004257 [PubMed: 19165335]

Yarkoni T, Braver TS, 2010 Cognitive neuroscience approaches to individual differences in working memory and executive control: Conceptual and methodological issues, in: Gruszka A, Matthews G,SB (Ed.), Handbook of Individual Differences in Cognition. Springer, New York, pp. 87–107. doi.org/10.1007/978-1-4419-1210-7_6

Yeo BT, Krienen FM, Sepulcre J, Sabuncu MR, Lashkari D, Hollinshead M, Roffman JL, Smoller JW, Zöllei L, Polimeni JR, Fischl B, Liu H, Buckner RL, 2011 The organization of the human cerebral cortex estimated by intrinsic functional connectivity. J. Neurophysiol. 106, 1125–1165. doi.org/10.1152/jn.00338.2011 [PubMed: 21653723]

Zelazo PD, Müller U, 2002 Executive function in typical and atypical development, in: Goswami U (Ed.), Blackwell Handbook of Childhood Cognitive Development. Blackwell, Malden, MA, pp. 445–469.

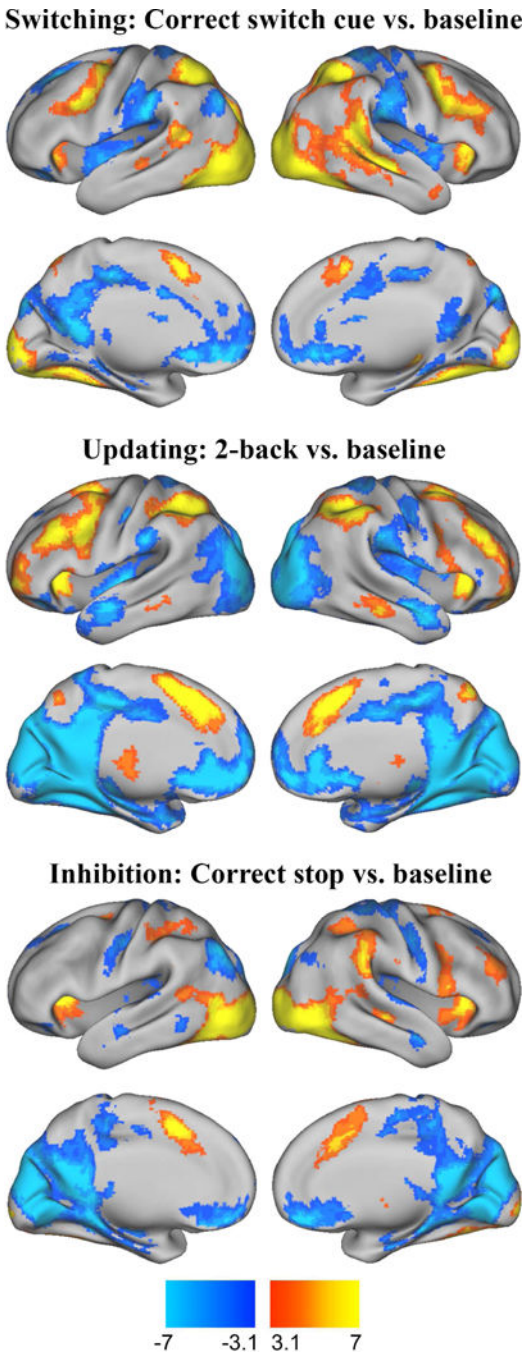

Figure 1.

Brain activity for switching, updating, and inhibition domains

Warm colors correspond to clusters for which percent signal change was significantly greater in the EF condition relative to baseline; cool colors correspond to clusters for which percent signal change was significantly lower in the EF condition relative to baseline. Maps were thresholded at $z > 3.1$ with a cluster probability of $p < .05$

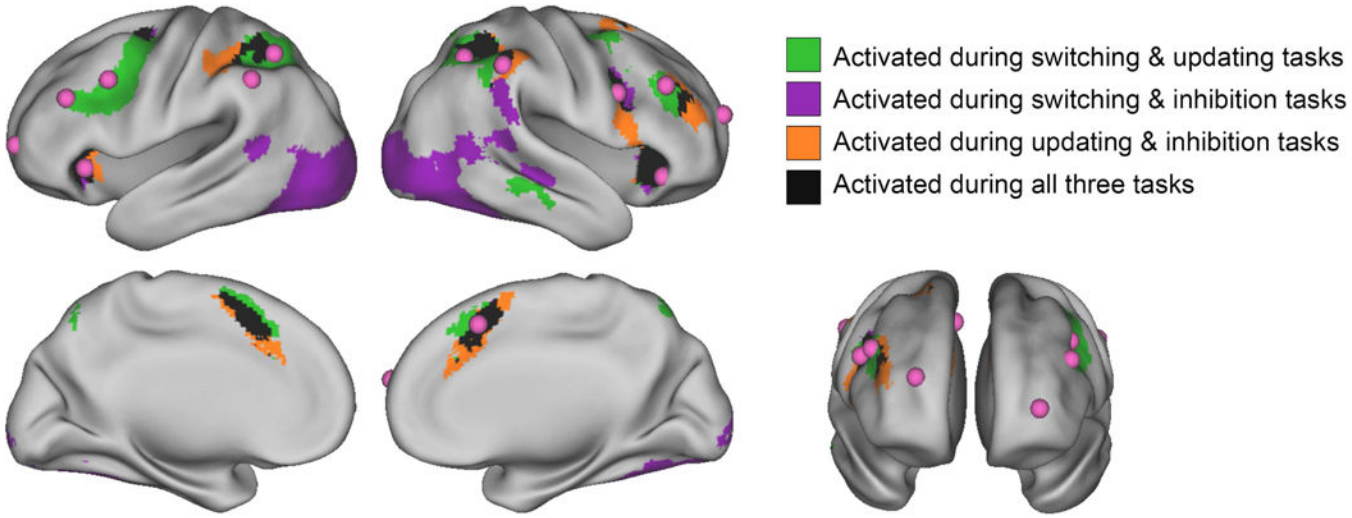

Figure 2.

Overlapping task-positive brain activity across three EF tasks, overlaid with adult ROIs Selected contrasts were *cue period during correct switch trials vs. baseline* for the switching task, *2-back blocks vs. baseline* for the updating task, and *correct stop trials vs. baseline* for the inhibition task. Prior to binarizing and summing across tasks, individual task maps were thresholded at $z > 3.1$ with a cluster probability of $p < .05$. Adult ROIs in pink were drawn from Dosenbach and colleagues (2006, 2010).

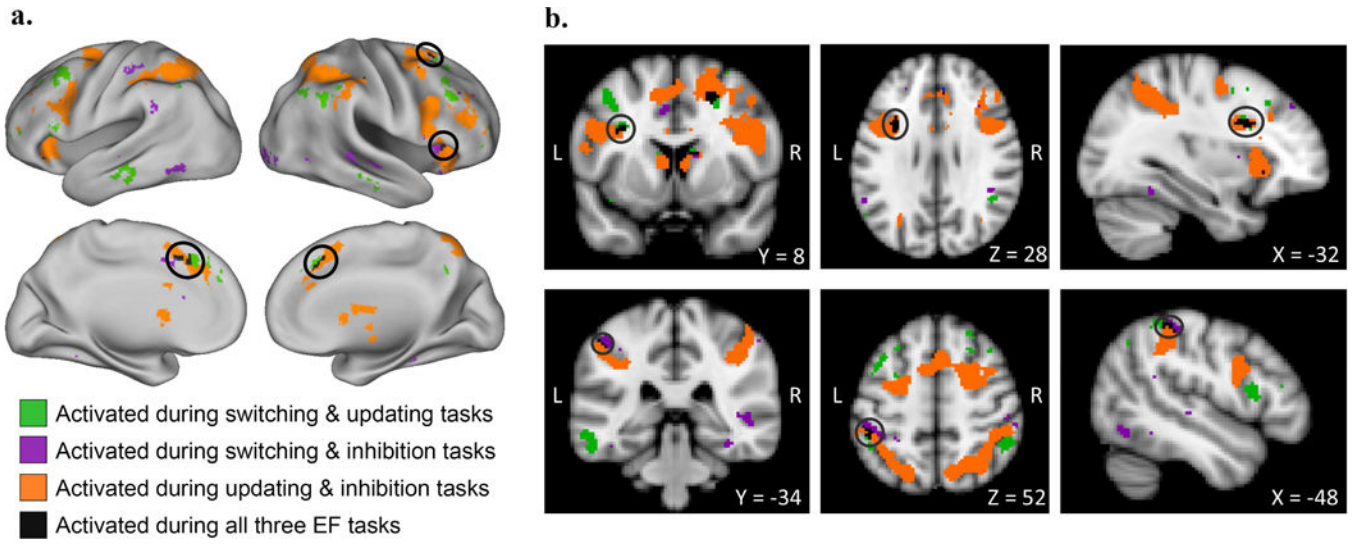

Figure 3.

Overlapping task-positive brain activity across stricter EF contrasts

Selected contrasts were *correct switch trials vs. correct repeat trials during the cue period* for the switching task, *2-back blocks vs. 1-back blocks* for the updating task, and *correct stop trials vs. correct go trials* for the inhibition task. Prior to binarizing and summing across tasks, individual task maps were thresholded at $z > 2.3$ with a cluster probability of $p < .01$. Circles in the top panel of (a) emphasize right frontal eye field and anterior insula clusters; those in the bottom panel of (a) emphasize the dorsal anterior cingulate cluster. Circles in the top panel of (b) emphasize the left inferior frontal sulcus cluster; those in the bottom panel of (b) emphasize the left IPL cluster. L = left, R = right.

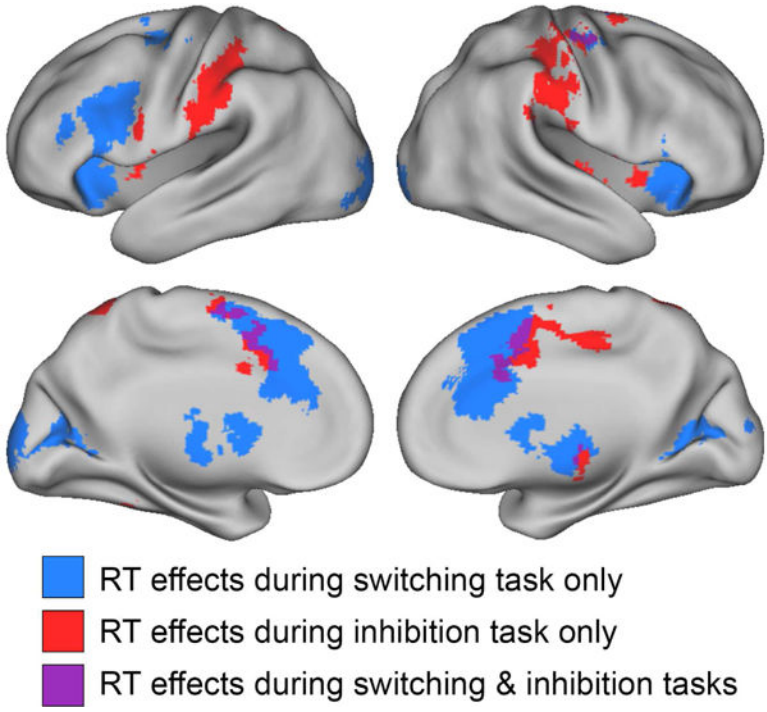

Figure 4.

Overlapping brain activity corresponding to response time across two EF tasks

The contrast applied to both tasks was *mean-centered response time vs. baseline*. Prior to binarizing and summing across tasks, individual task maps were thresholded at $z > 3.1$ with a cluster probability of $p < .05$.

Table 1.

Descriptive statistics for scanner performance

Performance measure	Description	*n*	*M*	*SD*	Range
Switching accuracy	Proportion correct	110	.84	.10	.62, 1.00
Switching RT	Mean RT, correct trials	110	1.11s	.15	.79, 1.42
Updating accuracy	Hits minus false alarms	100	7.71	3.95	−8, 13
Updating RT	Mean RT, correct trials	100	.84s	.16	.50, 1.33
Inhibition accuracy	Proportion correct, go trials	100	.87	.08	.71, .99
Inhibition RT	Stop signal RT	100	.25s	.05	.14, .39

RT = response time.

Table 2.

Task-overlapping centers of activity for EF contrasts

Region	MNI coordinates			Cluster size (voxels)
	x	y	z	
Dorsal anterior cingulate cortex	0	11	48	638
Center anterior insula	−31	20	3	243
Right anterior insula	35	20	3	480
Right dorsolateral prefrontal cortex	37	33	28	107
Right middle frontal gyrus, posterior aspect	44	6	32	149
Center frontal eye field	−25	−5	51	127
Right frontal eye field	26	−1	49	32
Center inferior parietal lobule, supramarginal gyrus	−45	−39	43	75
Right inferior parietal lobule, supramarginal gyrus	49	−41	47	118
Center superior parietal lobule	−30	−49	45	234
Right superior parietal lobule	33	−48	46	401

Cluster size and coordinates were determined by applying the FSL *cluster* command to the summed activation map. We report cortical clusters comprising 20 voxels or more. Voxel size: 2×2×2mm.

Table 3.

Task-overlapping centers of activity for stricter EF contrasts

Region	MNI coordinates			Cluster size (voxels)
	x	y	z	
Dorsal anterior cingulate cortex	−1	21	42	80
Right anterior insula, superior aspect	34	18	5	29
Right anterior insula, inferior aspect	36	18	−11	20
Right frontal eye field	22	7	48	36
Center inferior frontal sulcus	−33	9	28	36
Center inferior parietal lobule, supramarginal gyrus	−45	−42	54	32

Cluster size and coordinates were determined by applying the FSL *cluster* command to the summed activation map. We report cortical clusters comprising 20 voxels or more. Voxel size: 2×2×2mm.

Table 4.

Task-overlapping centers of activity for response time contrasts

Region	MNI coordinates			Cluster size (voxels)
	x	y	z	
Dorsal anterior cingulate cortex	0	6	47	421
Center thalamus	12	−16	9	48
Center precentral gyrus (primary motor cortex), lateral portion	37	−17	55	46
Center superior frontal gyrus, posterior portion	12	−1	65	20

Cluster size and coordinates were determined by applying the *cluster* command in FSL to the summed activation mask. We report clusters comprising 20 voxels or more. Voxel size: 2×2×2mm.